Journal of the Serbian Chemical Society
JSCS-info@shd.org.rs • www.shd.org.rs/JSCS
J. Serb. Chem. Soc. 76 (8) 1139–1152 (2011)
JSCS–4191
UDC 544.478+546.92:546.882+546.82+66.094.1:621.352
Original scientific paper

A novel platinum-based nanocatalyst at a niobia-doped titania support for the hydrogen oxidation reaction

NEVENKA R. ELEZOVIĆ[1*#], BILJANA M. BABIĆ[2], VELIMIR RADMILOVIĆ[3], LJILJANA M. GAJIĆ-KRSTAJIĆ[4], NEDELJKO V. KRSTAJIĆ[5] and LJILJANA M. VRAČAR[5]

[1]Institute for Multidisciplinary Research, University of Belgrade, Kneza Višeslava 1, 11030 Belgrade, [2]Vinča Institute of Nuclear Sciences, P. O. Box 522, 11001 Belgrade, Serbia, [3]National Center for Electron Microscopy, LBNL University of California, Cyclotron Road CA 94720 - Berkeley, USA, [4]Institute of Technical Sciences-SASA, Knez Mihailova 35, Belgrade and [5]Faculty of Technology and Metallurgy, University of Belgrade, Karnegijeva 4, 11000 Belgrade, Serbia

(Received 26 August 2010, revised 15 January 2011)

Abstract: The kinetics of the hydrogen oxidation reaction (HOR) was studied at Pt nanoparticles supported on niobia-doped titania (Pt/N–T). The catalyst support, with the composition of $0.05NbO_{2.5-\delta}$–$0.995TiO_2$ ($0 < \delta < 1$), was synthesized by a modified sol–gel procedure and characterized by the BET and X-ray diffraction (XRD) techniques. The specific surface area of the support was found to be 70 m^2 g^{-1}. The XRD analysis revealed the presence of the anatase TiO_2 phase in the support powder. No peaks indicating the existence of Nb-compounds were detected. Pt/N–T nanocatalyst was synthesized by the borohydride reduction method. Transmission electron microscopy revealed a quite homogenous distribution of the Pt nanoparticles over the support, with a mean particle size of about 3 nm. The electrochemical active surface area of Pt of 42±4 m^2 g^{-1} was determined by the cyclic voltammetry technique. The kinetics of the HOR was investigated by linear sweep voltammetry at a rotating disc electrode in 0.5 mol dm^{-3} $HClO_4$ solution. The determined value of the Tafel slope of 35 mV dec^{-1} and an exchange current density of 0.45 mA cm^{-2} per real surface area of the Pt are in good accordance with those already reported in the literature for the HOR at polycrystalline Pt and Pt nanocatalysts in acid solutions. This new catalyst exhibited better activity for the HOR in comparison with Pt nanocatalyst supported on Vulcan® XC-72R high area carbon.

Keywords: niobia-doped titania support; Pt nanocatalyst; hydrogen oxidation reaction; fuel cell.

* Corresponding author. E-mail: nelezovic@tmf.bg.ac.rs
# Serbian Chemical Society member.
doi: 10.2298/JSC100823100E

INTRODUCTION

In spite of the fact that proton exchange membrane fuel cells (PEMFCs) are promising future energy providers, many requirements regarding both the catalyst support and the catalyst material remain still unresolved. The main goals of contemporary research in this field are the development of inexpensive electrocatalysts for anode and cathode reactions, with high activity and satisfactory corrosion and chemical stability.

Platinum and Pt-based catalysts have been recognized as excellent catalysts for the hydrogen oxidation reaction.[1–3] The role of the supporting material for the functioning of a catalyst is very important, as it could affect both the catalytic activity and the durability of the catalyst. The catalyst support properties should be a combination of high surface area, excellent chemical stability and corrosion resistance. Hitherto, the most widely used supporting materials for Pt-based catalysts for the hydrogen oxidation reaction were carbon-based supports.[4–7] Carbon-based supports provide high electronic conductivity, an adequate physical surface for the dispersion of nanoparticles that is necessary to achieve a high surface area, also diminishing the catalyst loading. However, corrosion of a carbon support that could proceed either during recharge of a regenerative fuel cell at the air electrode at high overpotentials, or by start/stop of a simple fuel cell[8] is one of the main factors that could decrease the life time of PEMFCs. In the presence of water, carbon can also be consumed through the heterogeneous reaction: $C + H_2O \rightarrow H_2 + CO$,[9] especially in the presence of Pt which catalyses this reaction. The reaction product CO might poison the Pt catalyst. The above-mentioned disadvantages of carbon-based supports imply the need for new supporting materials, in order to prevent damage of the Pt nanocatalysts, enhance the reliability and reduce the total lifetime costs of PEMFC.

Several titanium oxide phases, mainly Ti_4O_7 and Ti_5O_9, known as Magneli phases, have been reported as promising catalyst supports for Pt-based nanocatalysts, for electrochemical reactions in PEMFCs.[10–12] The main disadvantage of the above-mentioned titanium oxides as supporting materials are their very low specific surface area. Namely, the maximum obtained value of the surface area is too low to achieve high dispersion and compositional homogeneity of the Pt nanoparticles over the support, which are important requirements for enhanced electrocatalytic activity. Ioroi *et al*. reported good corrosion stability of a Ti_4O_7-supported Pt catalyst, as well as almost the same catalytic activities as the XC-72/Pt catalyst for both the hydrogen oxidation reaction and the oxygen reduction reaction.[13]

According to the literature,[14] niobium oxide nanoparticles could be a promising material for catalyst support for Pt-based nanaocatalysts, owing its excellent chemical stability in acid solutions.

The aim of this work was to test a Pt nanocatalyst supported on a novel niobia-doped titania support (Pt/N–T) for the hydrogen oxidation reaction (HOR) and to compare the obtained results with those already reported for carbon-supported Pt-based nanocatalysts. A support with the composition $0.05NbO_{2.5-\delta}$–$–0.995TiO_2$ ($0 < \delta < 1$) was synthesized and completely characterized by the nitrogen adsorption/desorption isotherm and X-ray diffraction (XRD) techniques. A Pt nanocatalyst was synthesized on this support using the borohydride reduction method and characterized by the transmission electron microscopy (TEM) technique. This catalyst has already been tested for the oxygen reduction reaction and enhancements of the specific and mass activities were found.

EXPERIMENTAL

Synthesis of N–T support

The N–T support was synthesized by a modified sol–gel procedure proposed by Boujday *et.al*.[15] This procedure considers the acid-catalyzed sol–gel method in a non-aqueous medium. The sol was prepared by adding 0.9 ml of a 37 % solution of hydrochloric acid (Zorka, Serbia) to 40 ml of a 97 % solution of titanium tetra-isopropoxide, $Ti(O–iPr)_4$ (Alfa Aesar, Germany), and the appropriate volume of 0.17 ml of 99.95 % niobium(V) ethoxide (Aldrich, Germany) under vigorous stirring (0.5 % Nb in a Nb/Ti atomic ratio to obtain a $Nb_{0.005}Ti_{0.995}O_2$ solid solution). Finally, 4.8 ml of deionized (D.I.) water was added under continuous stirring. The mixture was placed in glass tubes, sealed and left at room temperature for 5 days. In the presence of such an amount of hydrochloric acid, the hydrolysis proceeded without the formation of a precipitate, leading to a transparent sol. Gellification of the sol was achieved by adding an appropriate amount of water.

The sample was freeze-dried using a Modulyo Freeze Dryer System, Edwards, England, consisting of a freeze dryer unit and a high vacuum pump E 2 M 8, Edwards. The sample was pre-frozen in a freezer at –30 °C for 24 h. Subsequently, the sample was freeze-dried in the acrylic chamber with the shelf arrangements mounted directly on the top of the condenser of the freeze dryer. The vacuum during the twenty-hour freeze-drying was around 4 mbar. The dried sample was heated at 400 °C for 2 h in a conventional furnace to obtain crystallized anatase phase and to remove traces of organics. After the treatment, the furnace was cooled to room temperature. Finally, to activate the Nb-donor dopant in the TiO_2, the nanoparticles were additionally annealed at 400 °C for 2 h under a pure H_2 gas flow and cooled to room temperature under a H_2 gas atmosphere.[16]

Synthesis of the Pt/N–T catalyst

The Pt/N–T catalyst containing 20 mass % Pt was prepared by means of the borohydride reduction method.[16] An appropriate amount of H_2PtCl_6 was dissolved in D.I. water. The support powder was dispersed in D.I. water and then the metal salt solution was added under constant stirring. The mixture of metal salt and the support was reduced by using an excess of sodium borohydride solution. The precipitate was washed with D.I. water and then dried at 80 °C.

The Pt/XC catalyst (with a real active Pt surface area of 96 $m^2\ g^{-1}$, determined by cyclic voltammetry), which was used for comparison of the activities for the HOR, was synthesized by a modified ethylene glycol method on commercial carbon (Vulcan XC-72R) support. The details of the synthesis have already been reported.[5]

Cell and electrode preparation

Pt/N–T catalyst (20 mg) was ultrasonically suspended in 9.5 ml of water and 0.5 ml of Nafion solution (5 mass %, Aldrich solution) to prepare a catalyst ink. Then, 20 μl of ink was transferred with an injector to a gold disk electrode (5 mm diameter). After volatilization of the water, the electrode was heated at 80 °C for 10 min. The so-prepared electrodes were always characterized by cyclic voltammetry in order to confirm their similar real Pt surface area (estimated from the H underpotential deposition (upd) region). The reproducibility (10 %) of the determined real Pt surface area was very good; hence, the amount of Pt on the electrode was considered to be 8.0±0.8 μg.

For the electrochemical measurements, a conventional rotating disk electrode (RDE) three-compartment cell was used. The working electrode compartment was separated from the other two compartments by fritted glass discs. The counter electrode was a platinum sheet of 5 cm^2 geometric area. All measurements were performed with a Pt/H_2 reference electrode (RHE) in the same solution, at the same temperature as the working electrode. The RHE was kept in a compartment separated from the working electrode by a wetted, closed glass stopcock and purified hydrogen was bubbled continuously through the solution.

Electrode characterization

Adsorption and desorption isotherms. The nitrogen adsorption and desorption isotherms were measured on the N–T support at –196 °C, using the gravimetric McBain method. The specific surface area, S_{BET}, and the pore size distribution were calculated from the isotherms. Pore size distribution was estimated by applying the Barrett–Joyner–Halenda (BJH) method.[17]

XRD Analysis. Structural analysis (XRD) was realized using a Siemens D-500 diffractometer. Cu Kα radiation was used in conjunction with a Cu Kβ nickel filter. The XRD pattern was used to evaluate the crystallite size of the Nb–TiO_2 support. The average crystallite size, *D*, was calculated from the Scherrer formula: $D = 0.9\lambda/\beta\cos\theta$, where λ is the wavelength of the X-rays, θ is the diffraction angle, $\beta = (\beta_m^2 - \beta_s^2)$, β is the corrected half-width, β_m the observed half-width and β_s is the half-width of a standard Si sample (provided by Siemens).

TEM Measurements. Transmission electron microscopy (TEM) measurements were performed at the National Center for Electron Microscopy (NCEM-Berkeley) using a FEI (Fillips electronic instruments)-CM200 super-twin and CM300 ultra-twin microscopes operating at 200 and 300 kV and equipped with Gatan 1k×1k and 2k×2k CCD cameras, respectively. Specimens were prepared for TEM by making suspensions of the catalyst powder in ethanol, using an ultrasonic bath. These suspensions were dropped onto clean holey carbon grids, and then air-dried.

The particle size distribution was determined from images of, on average, 20 different regions of the catalyst; each region contained 10–20 particles. The particle shapes were determined by real space crystallography with the use of high-resolution images taken from particles near or on the edge of the N–T substrate, and/or by numerical Fourier filtering of the digitized image intensity spectrum of particles on top of the support.

Electrochemical characterization. The cyclic voltammetry experiments were performed in the potential range between hydrogen and oxygen evolution (0.04–1.4 V *vs.* RHE), in 0.5 mol dm^{-3} $HClO_4$ solution, with various scan rates at the Pt/N–T and Pt/XC electrodes. Prior to recording the cyclic voltammograms, the electrode surface was stabilized by repetitive cycling from 0.04 to 1.4 V *vs.* RHE. The solution ($HClO_4$, Spectrograde, Merck) was prepared in D.I. water ("Millipore"– 18 MΩ cm resistivity), at a temperature of 25 °C, which was saturated with high purity nitrogen by continuously bubbling through the working electrode compartment during the experiments.

Linear sweep voltammetry curves for the HOR in 0.5 M $HClO_4$ solution saturated with pure hydrogen, continuously bubbling through the working electrode compartment, were recorded at 10 mV s^{-1} sweep rate. A PAR universal programmer, model 175, was used to provide the potentiodynamic voltage time program addressed to a PAR model 371 potentiostat/ /galvanostat.

RESULTS AND DISCUSSION

BET and XRD analysis of N–T support

The nitrogen adsorption isotherm for the N–T support, according to the IUPAC classification, belongs to type IV, associated with mesoporous materials. The specific surface area of the support powder calculated by the BET equation was determined to be 70 m^2 g^{-1}. The pore size distribution is presented in Fig. 1.

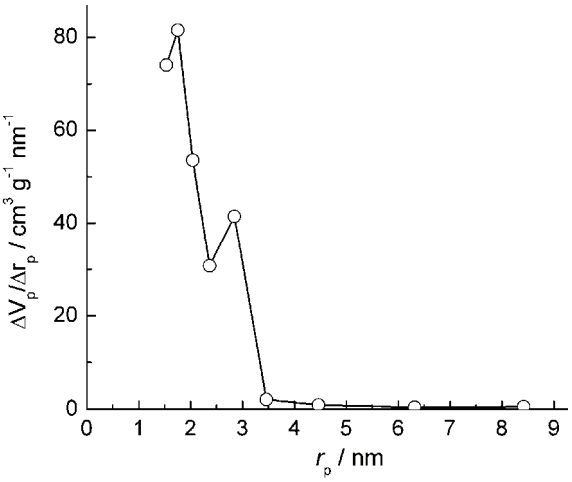

Fig. 1. Pore size distribution for the N–T support.

The X-ray pattern of the N–T support sample is shown in Fig. 2. It could be seen that all peaks present belong to the anatase phase of titanium dioxide. No peaks corresponding to niobium compounds were detected. The broad peaks indicate to nano-sized particles. The obtained values for lattice parameters were $a = b = 0.37854$ nm and $c = 0.94835$ nm. The determined values of the lattice parameters for anatase titanium oxide were enlarged compared to those of pure anatase (JCPDS 21-1272), indicating niobium incorporation into the lattice. It is well known that Nb (or V and Ta) can be substitutionally incorporated within the TiO_2 lattice.[18,19] Investigation of the structural properties of niobia-doped titania even up to 38 % of Nb, showed the existence of only a pure anatase or rutile phase, depending on the growth temperature.[20] In the present study, in order to activate the Nb-donor dopant in TiO_2, the nanoparticles were additionally annealed at 400 °C and XRD analysis showed the existence of anatase TiO_2. This result is in good accordance with literature results which reported that up to 550

°C, only anatase was present, while at 800 °C and higher, pure rutile phase was obtained.[20]

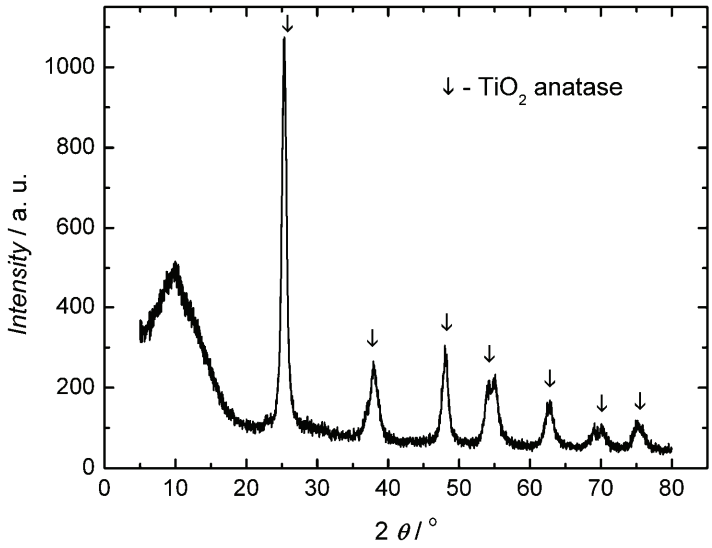

Fig. 2. XRD Diffraction results for the N–T support.

TEM Analysis of the Pt/N–T catalyst

TEM Micrographs of the N–T-supported Pt nanocatalyst are presented in Fig. 3. Figure 3a shows a low-magnification transmission electron micrograph of

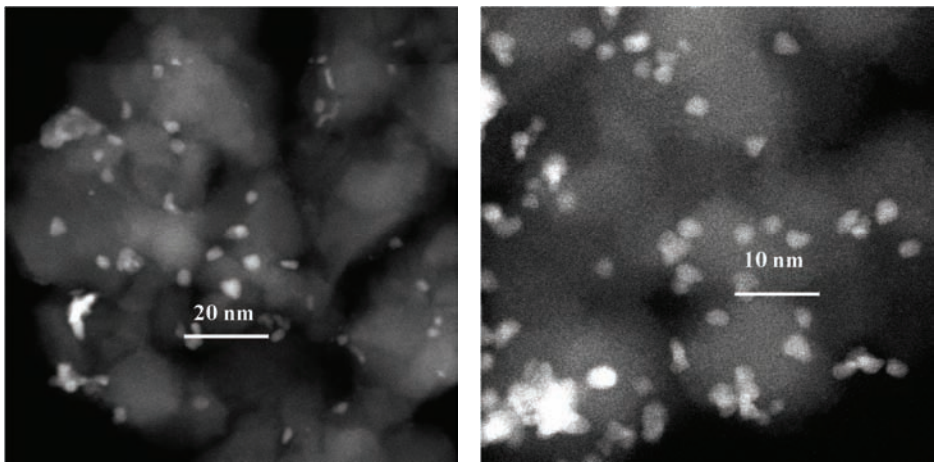

(a) (b)

Fig. 3. TEM micrographs of the Pt/N–T nanocatalyst: a) low magnification image showing a homogeneous distribution of Pt particles on the catalyst support; b) high resolution dark field image of the catalyst, showing no pronounced agglomeration of the particles.

the Pt nanoparticles on the N–T support. It is evident that the Pt nanoparticles are globular in shape and quite uniformly distributed over the N–T support. Using these results, it was possible to determine the Pt particle size distribution, as well as to calculate the total surface area of the particles by analyzing the images from different regions of the catalyst, taking into account the hypothesis that all the particles are globular in shape and have the same average particle size. A high resolution electron microscopy image of the Pt/N–T sample is shown in Fig. 3b. There is no evidence of pronounced particle agglomeration. The determined average size of the nanoparticle was about 3 nm.

Cyclic voltammetry results

The cyclic voltammetry responses at the N–T support, and the Pt/N–T and the Pt/XC nanocatalysts were recorded in the potential range between oxygen and hydrogen evolution in 0.5 mol dm^{-3} $HClO_4$ solution. The obtained results are presented in Fig. 4. The cyclic voltammetry response of the N–T support (Fig. 4 inset) shows the rectangular shape that is expected for an ideal electrochemical double-layer capacitor. No significant peaks revealing the presence of oxidative–reductive processes were observed. This result proves that N–T was an electrochemically inert support over the whole range of applied potential (0.04––1.40 V *vs*. RHE). The cyclic voltammetric curve of the Pt/N–T electrode (Fig.

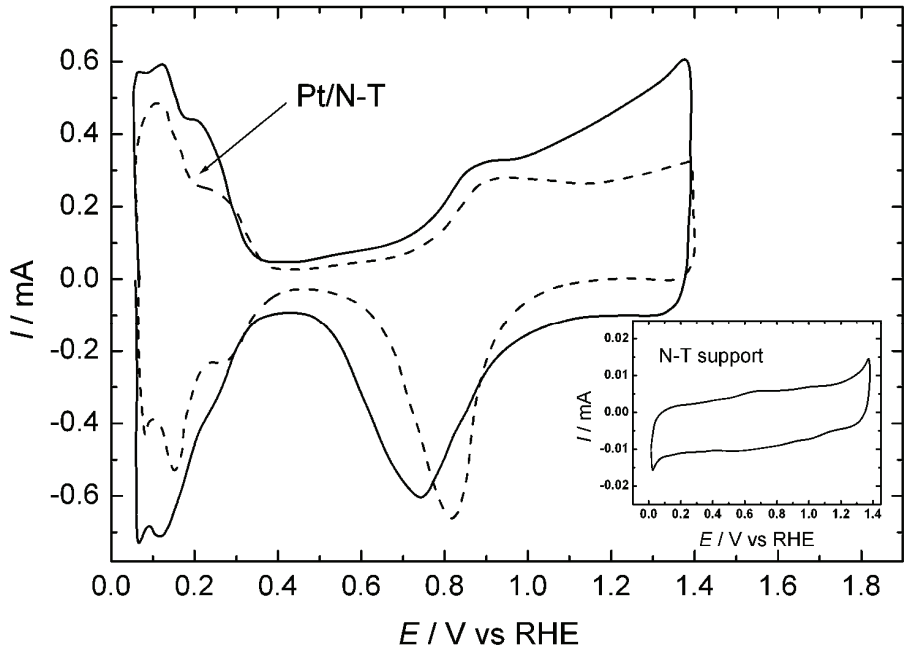

Fig. 4. Cyclic voltammograms obtained at the N–T support, and the Pt/N–T and Pt/XC nanocatalysts in nitrogen-purged, 0.5 mol dm^{-3} $HClO_4$, using a 0.1 V s^{-1} sweep rate, at 25 °C.

4), in the same solution saturated with N_2, has a typical voltammogram shape for Pt in acid solution, with very clear hydrogen adsorption–desorption and PtOH formation and reduction regions. The cyclic voltammogram of the Pt/XC nanocatalyst, under the same experimental conditions, is also presented in Fig. 4. A similar Pt-like shape could be observed and a lower specific surface area of Pt in the Pt/N–T catalyst, estimated based on the desorption charge of hydrogen in the under potential deposition region. The Pt/N–T catalyst in comparison with the Pt/XC was also characterized by a very narrow, symmetric double layer region, as a consequence of its lower capacitance current contribution.

The electrochemically active surface area of Pt for the Pt/N–T catalyst was determined from the adsorption/desorption charge of hydrogen atoms, after subtraction of the double layer charge, taking the reference value of 210 μC cm^{-2} for a charge of full coverage with adsorbed hydrogen species at Pt.[21] This calculation gave the value of specific electrochemical active area of 42±4 m^2 g^{-1} Pt for the Pt/N–T electrode.

Hydrogen oxidation reaction at Pt/N–T electrode

It is well known that hydrogen oxidation on Pt-based electrodes in acid solution is one of the fastest electrochemical reactions. The measured currents reach the diffusion limitation rising to the diffusion-limited level within less than 0.10 V *vs*. RHE, even at a RDE. For this reason, the mixed controlled potential region must be analyzed in order to collect kinetic information from experimentally obtained results.

The basic assumption of the analysis is that the measured current is determined by the overall resistance that consists of three components: one related to electron transfer kinetics, the two others result from mass transport limitations. According to this, the kinetically controlled current, I_k, at a given potential E can be determined from RDE curves using the equation proposed by Lawson:[22]

$$\frac{1}{I} = \frac{1}{I_k} + \frac{1}{I_L} + \frac{1}{I_f} \tag{1}$$

and

$$I_L = 0.62nFD^{2/3}c\nu^{-1/6}\omega^{1/2} \tag{2}$$

where I_k is the kinetic current in the absence of any mass-transfer effects, and I_L is the so-called Levich current, controlled mainly by diffusion. Other parameters have their usual significance in the conventional Levich Equation. I_f represents the diffusion current controlled by reactant diffusion through the Nafion film and is equal to:

$$I_f = nFD_f c_f L^{-1} \tag{3}$$

where D_f, c_f and L stand for the diffusion coefficient and the concentration of dissolved hydrogen in the Nafion film, and the film thickness, respectively. At a sufficiently large potential, E, and if the rotation rate of the electrode is increased enough ($\omega \to \infty$), the kinetic current, I_k and I_L become very large and under such conditions, the measured current I is equal to I_f. Based on the above consideration, it is possible to obtain the value of I_f from the intercept of $1/I_{L.lim}$ axis by extrapolating the relationship of $1/I_{L.}$ *vs.* $\omega^{-1/2}$, where $I_{L.lim}$ represents the diffusion-limited current density at a given rotation rate.

The potentiodynamic curves for the oxidation of H_2 on the Pt/N–T electrode at different rotation rates in 0.5 mol dm^{-3} $HClO_4$ solution at 25 °C are presented in Fig. 5. It can be seen that the HOR starts at 0.0 V *vs.* RHE and reach the diffusion-limited current at approximately 0.05 V. Linear sweep voltammograms for the HOR at two different rotation rates for the Pt/XC and Pt/N–T electrodes are presented in Fig. 6. Although very similar values of currents were observed, Pt/N–T catalyst is characterized by a higher specific activity for the HOR, expressed in terms of the current density, taking into account its lower real surface area, determined by cyclic voltammetry. It should be mentioned that it is not common to refer to catalytic activity for the HOR at Pt based catalyst in terms of current density value at any given potential, as it is usually reported for the oxygen reduction reaction.

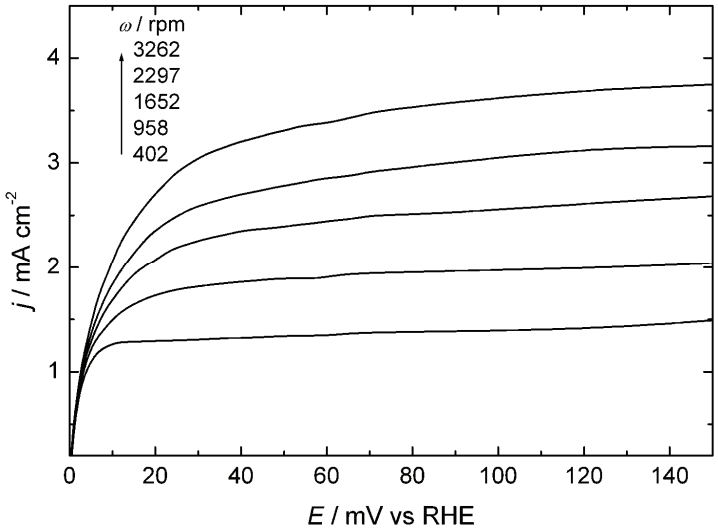

Fig. 5. Linear-sweep voltammograms for the HOR at the Pt/N–T nanocatalyst (current density expressed per geometric surface area), for different rotation rates in 0.5 mol dm^{-3} $HClO_4$ solution saturated with pure H_2 (scan rate 0.01 V s^{-1}) at 25 °C.

A Levich–Koutecky plot based on the experimental data at 0.15 V is shown in Fig. 7. The value of the current density controlled by diffusion of the reactant

through the Nafion film, determined from the intercept in Fig. 6, was about 55 mA cm^{-2} (the current density is expressed per geometric surface area). Nevertheless, its contribution to the measured current densities is negligible if the values of I_k determined from Eq. (1) are less than 10 % of the minimum value of I_f. This means that is not possible to obtain accurately a polarization curve for the HOR from the corresponding modified Levich–Koutecky plots.

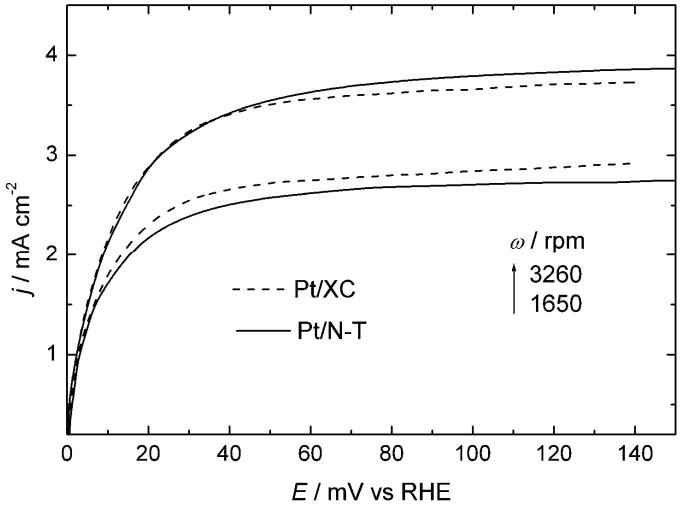

Fig. 6. Linear sweep voltammograms for the HOR at the Pt/N–T and Pt/XC nanocatalysts (current density expressed per geometric surface area) at two different rotation rates in 0.5 mol dm^{-3} $HClO_4$ solution saturated with pure H_2 (scan rate 0.01 V s^{-1}) at 25 °C.

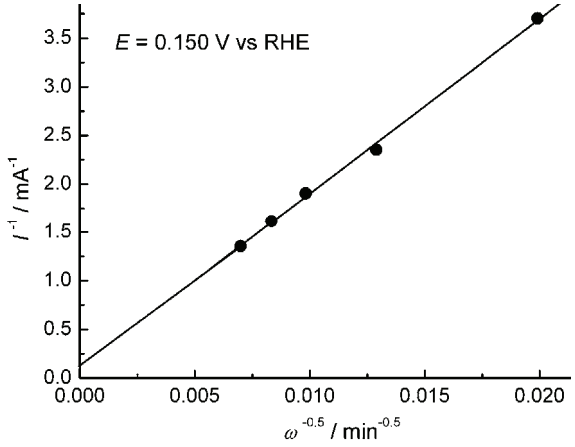

Fig. 7. Levich–Koutecky plot for the HOR at a Pt/N–T RDE in 0.5 mol dm^{-3} $HClO_4$ solution at 25 °C, in the diffusion-limited potential region at E = 0.15 V *vs.* RHE.

Tafel plots are commonly used to obtain kinetic information for the HOR.[1,23,24] A summary of the theoretically predicted values of the Tafel slopes

for different types of mechanisms for the HOR at platinum electrodes in acid solutions are presented in Table I. For the HOR on platinum electrodes, the most widely accepted mechanism is chemical adsorption (Tafel step) or electrochemical adsorption (Heyrovsky step), followed by adsorbed hydrogen discharge (Volmer step), as is presented by the following equations:[3]

$$H_2 + 2M \rightarrow 2MH \quad \text{(Tafel step)} \quad (4)$$

$$H_2 + M \rightarrow MH + H^+ + e^- \quad \text{(Heyrovsky step)} \quad (5)$$

$$MH \rightarrow M + H^+ + e^- \quad \text{(Volmer step)} \quad (6)$$

TABLE I. Theoretical values of the Tafel slopes ($b = 2.303RT/\beta F$) and mechanisms for the HOR in acid solutions at 25 °C

Mechanism	b / mV dec^{-1}	Rate-determining step
Tafel–Volmer	30	Tafel
Heyrovsky–Volmer	118	Heyrovsky
Tafel–Volmer and Heyrovsky–Volmer	59	Volmer

In order to obtain information about the kinetics of the HOR at the Pt/N–T catalyst, the RDE polarization data were analyzed in terms of mass transport corrected Tafel diagrams and the obtained results are presented in Fig. 8.

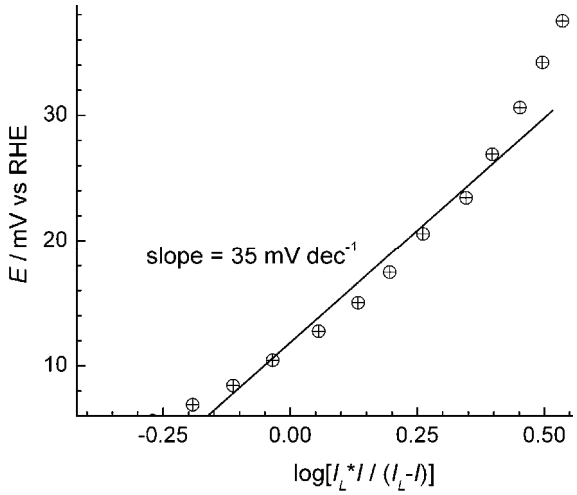

Fig. 8. Mass corrected Tafel plot for the HOR at a Pt/N–T RDE in 0.5 mol dm^{-3} $HClO_4$, at 25 °C.

The Tafel slope of 35 mV dec^{-1} is in good accordance with the already reported slope for the hydrogen oxidation reaction at platinum single crystals,[23] smooth platinum[25] and platinum nanocatalysts in acid solutions.[3,5]

It is not possible to determine the exchange currents (I_0) simply by extrapolating the Tafel lines to the reversible potential due to the absence of a well-defined Tafel region. The exchange current was estimated from the slope of the

linear polarization response and after correction for diffusion, using the following equation:[5]

$$\frac{\Delta E}{\Delta I} = \frac{RT}{nF}\left(\frac{1}{I_0} + \frac{1}{I_{\mathrm{L,lim}}}\right) \tag{7}$$

where $n = 2$ and $I_{\mathrm{L,lim}}$ is the limiting current.

This calculation assumes that the HOR and the hydrogen evolution reaction (HER) follow the same reaction mechanism around the equilibrium potential. The obtained value for the exchange current density of 0.45 mA cm^{-2} is in good accordance with previously reported values for the HOR at Pt in acid solutions,[23,26] determined using the RDE technique. The determined exchange current density, expressed per real surface area, is twice as high as that obtained for the HOR at a Pt nanocatalyst on a carbon support.[5]

This new catalyst was already tested for the oxygen reduction reaction and a five times enhancement in the catalytic activity per mass Pt loaded, as well as ten times enhancement in the specific activity (per real electrochemically active surface area) were reported.[27] Bearing in mind that the overall cell performance in PEMFCs is influenced much more by the oxygen reduction reaction, owing to its much higher overvoltage compared with the hydrogen oxidation reaction, it could be concluded that this new catalyst is promising for applications in PEMFCs.

CONCLUSIONS

An N–T support was successfully synthesized by a modified sol–gel procedure. The specific surface area of the support, determined by the BET technique, was found to be 70 $m^2\ g^{-1}$. The presence of anatase TiO_2 in the synthesized catalyst support powder was determined by XRD measurements. No peak corresponding to Nb-compounds was detected.

A Pt/N–T nanocatalyst was successfully synthesized by the borohydride reduction method. TEM Analysis revealed a quite homogenous distribution of Pt nanoparticles on the N–T support, with an average particle size of about 3 nm.

The electrochemically active surface area of the Pt in the Pt/N–T nanocatalyst, determined by the cyclic voltammetry technique, was found to be 42±4 $m^2\ g^{-1}$.

Electrochemical characterization of the fabricated catalyst for the HOR revealed a Tafel slope of 35 mV dec^{-1} and an exchange current density of 0.45 mA cm^{-2}. This value of the Tafel slope and the exchange current density are of the same order of magnitude already accepted in literature for the HOR at a platinum-based catalyst in acid solutions. The determined exchange current density was two-times higher than the corresponding value obtained for the hydrogen oxidation reaction at a Pt carbon supported catalyst.

Acknowledgments. The authors are indebted to the Ministry of Education and Science of the Republic of Serbia for the financial support under Contract No. 172054. Velimir Radmilović acknowledges support by the United States Department of Energy under Contract #DE--AC02-05CH11231.

ИЗВОД

НОВИ Pt КАТАЛИЗАТОР НА НОСАЧУ НА БАЗИ TiO_2 ЗА РЕАКЦИЈУ ОКСИДАЦИЈЕ ВОДОНИКА

НЕВЕНКА Р. ЕЛЕЗОВИЋ[1], БИЉАНА М. БАБИЋ[2], ВЕЛИМИР РАДМИЛОВИЋ[3], ЉИЉАНА М. ГАЈИЋ-КРСТАЈИЋ[4], НЕДЕЉКО В. КРСТАЈИЋ[5] и ЉИЉАНА М. ВРАЧАР[5]

[1]Институт за мултидисциплинарна истраживања, Универзитет у Београду,Кнеза Вишеслава 1, 11030 Београд, [2]Институт за нуклеарне науке Винча, п. пр. 522, Београд, [3]National Center for Electron Microscopy, LBNL University of California, Cyclotron Road, CA 94720- Berkeley, USA, [4]Институт техничких наука САНУ, Кнез Михаилова 35, 11000 Београд и [5]Технолошко–металуршки факултет Универзитета у Београду, Карнегијева 4, Београд

Кинетика електрохемијске оксидације водоника је испитивана на Pt нанокатализатору на носачу састава $0{,}05NbO_{2{,}5-\delta}$–$0{,}995TiO_2$ ($0 < \delta < 1$) (у тексту Pt/N–T). Носач катализатора је синтетисан применом модификованог сол–гел поступка и окарактерисан BET методом и методом дифракције X-зрака. Специфична површина носача је била 70 $m^2\ g^{-1}$. Дифракцијом X-зрака је утврђено присуство TiO_2 у форми анатаза, док пикови који би указивали на присуство једињења Nb нису детектовани. Нанокатализатор Pt/N–T је синтетисан методом редукције помоћу бор-хидрида. Применом трансмисионе електронске микроскопије је показана хомогена расподела наночестица Pt на носачу, са просечном величином честица око 3 nm. Применом цикличне волтаметрије је одређена електрохемијска активна површина катализатора приближне вредности 42±4 $m^2\ g^{-1}$. Кинетика реакције оксидације водоника је испитивана применом линеарне скенирајуће волтаметрије на ротирајућој диск електроди у раствору 0,5 mol dm^{-3} $HClO_4$. Добијене вредности Тафеловог нагиба и густине струје измене од 35 mV $дек^{-1}$ и 0,45 mA cm^{-2} (обрачунато по електрохемијски активној површини Pt) су у сагласности са литературним вредностима за реакцију оксидације водоника на поликристалној Pt и на наночестицама Pt у киселим растворима. Нови катализатор Pt/N–T је показао већу активност за оксидацију водоника од Pt нанокатализатора на носачу од угља развијене површине (Vulcan® XC-72R).

(Примљено 26. августа 2010, ревидирано 15. јануара 2011)

REFERENCES

1. R. M. Q. Mello, E. A. Ticianelli, *Electrochim. Acta* **42** (1997) 1031
2. J. Shim, C. R. Lee, H. K. Lee, J. S. Lee, E. J. Cairns, *J. Power Sources* **102 (**2001) 172
3. A. F. Innocente, A. C. D. Angelo, *J. Power Sources* **162** (2006) 151
4. S. J. Lee, S. Mukerjee, E. A. Ticianelli, J. McBreen, *Electrochim. Acta* **44** (1999) 3283
5. B. M. Babić, Lj. M. Vračar, V. Radmilović, N. V. Krstajić, *Electrochim. Acta* **51** (2006) 3820
6. R. B. Lin, S. M. Shih, *J. Chin. Inst. Chem. Eng.* **38** (2007) 365
7. J. Kim, J. H. Jang, Y. H. Lee, Y. U. Kwon, *J. Power Sources* **193 (**2009) 441
8. C. A. Reiser, L. Bregoli, T. W. Patterson, S. Yi. Jung, J. D. Yang, M. L. Perry, T. D. Jarvi, *Electrochem. Solid-State Lett*. **8** (2005) A273
9. Y. Shao, G. Yin, Y. Gao, *J. Power Sources* **171** (2007) 558

10. G. R. Dieckmann, S. H. Langer, *Electrochim. Acta* **44 (**1998) 437
11. L. He, H. F. Franzen, J. E. Vitt, D. C. Johnson, *J. Appl. Electrochem.* **26** (1996) 785
12. E. E. Farndon, D. Pletcher, *Electrochim. Acta* **42** (1997) 1281
13. T. Ioroi, Z. Siroma, N. Fujiwara, S. Yamazaki, K. Yasuda, *Electrochem. Commun.* **7** (2005) 183.
14. K. Sasaki, L. Zhang, R. R. Adzic, *Phys. Chem. Chem. Phys.* **10** (2008) 159
15. S. Boujday, F. Wunsch, P. Portes, J. F. Bocquet, C. Colbeau-Justin, *Sol. Energ. Mat. Sol. C.* **83** (2004) 421
16. K. W. Park, K. S. Seol, *Electrochem. Commun.* **9** (2007) 2256
17. E. P. Barret, L. G. Joyner, P. P. Halenda, *J. Am. Chem. Soc.* **73** (1951) 373
18. D. Morris, Y. Dou, J. Rebane, C. E. J. Mitchell, R. G. Egdell, *Phys. Rev., B* **61** (2000) 13445
19. E. Antolini, E. R. Gonzalez, *Solid State Ionics* **180** (2009) 746
20. Y. Gao, *Thin Solid Films* **346** (1999) 73
21. J. T. Hwang, J. S. Chung, *Electrochim. Acta* **38** (1993) 2715
22. D. R. Lawson, L. D. White, C. R. Martin, M. N. Szentirmay, J. I. Song, *J. Electrochem. Soc.* **135** (1988) 2247
23. N. M. Markovic, B. N. Grgur, P. N. Ross, *J. Phys. Chem., B* **101** (1997) 5405
24. P. M. Quaiano, M. R. G. De Chialvo, A. C. Chialvo, *Phys. Chem. Chem. Phys.* **6** (2004) 4450
25. B. E. Conway, B. V. Tilak, *Electrochim. Acta* **47** (2002) 3571
26. N. R. Elezovic, B. M. Babic, V. R. Radmilovic, Lj. M. Vracar, N. V. Krstajic, *Phys. Chem. Chem. Phys.* **11** (2009) 5192
27. N. R. Elezovic, B. M. Babic, Lj. Gajic-Krstajic, V. Radmilovic, N. V. Krstajic, Lj. Vracar, *J. Power Sources* **195** (2010) 3961.